Computational Materials Science 98 (2015) 345–353

Contents lists available at ScienceDirect

Computational Materials Science

journal homepage: www.elsevier.com/locate/commatsci

A computational study of special grain boundaries in WC–Co cemented carbides

Sven A.E. Johansson, Martin V.G. Petisme, Göran Wahnström *

Department of Applied Physics, Chalmers University of Technology, SE-412 96 Göteborg, Sweden

ARTICLE INFO

Article history:
Received 18 August 2014
Received in revised form 13 November 2014
Accepted 15 November 2014

Keywords:
Cemented carbides
Grain boundary energy
Grain boundary segregation
Density functional theory

ABSTRACT

In this work, we model $\Sigma = 2$ and $\Sigma = 1$ $\{10\bar{1}0\}\|\{10\bar{1}0\}$ WC/WC boundaries in WC–Co using density functional theory (DFT). In particular, the misfit structure of the $\Sigma = 2$ twist boundary is modeled explicitly with a previously developed Peierls–Nabarro model for misfit dislocations. The grain boundary energy of the twist boundary is found to be 0.7 J/m^2, which is small in comparison with energies of general WC/WC boundaries. The misfit structure can be described as a square network of screw dislocations with Burgers vectors $\frac{1}{6}\langle 1\bar{2}13\rangle$. Our calculations show that Co will not segregate to the $\Sigma = 2$ twist boundary, which contrasts with predictions for other WC/WC boundaries that typically give half a monolayer of segregated Co.

1. Introduction

WC–Co based cemented carbides, or hardmetals are, from a technical point of view, one of the most successful composite materials [1,2]. They combine excellent hardness with high toughness, and are produced by sintering WC and Co powders at a temperature slightly above the melting temperature of Co. The hardness of the sintered material is provided by the carbide skeleton, whereas the toughness is provided by the ductile metal binder phase. In addition to the bulk phases, interfaces and grain boundaries have a major influence on final mechanical properties as well as on the sintering process.

Grain boundaries in cemented carbides have been characterized both in terms of atomic composition and structure [3–14] as well as geometric distribution [15–18]. Owing to the WC hexagonal lattice structure ($a = 2.906$ Å, $c = 2.837$ Å) with its c/a ratio of $0.976 \approx 1$, several near coincident site lattices (CSL) with low Σ are possible [3]. In particular, approximate $\Sigma = 2$ boundaries are possible, which can be thought of as formed by a 90° rotation of one grain around a common $[10\bar{1}0]$ direction [3,19]. Electron backscatter diffraction (EBSD) analyses of sintered WC–Co show that grain boundary misorientation distributions typically have a very distinct peak at 90°, which is due to the $\Sigma = 2$ boundaries [15–17]. These boundaries have therefore attracted considerable interest during the last decade.

It is now well-established that $\Sigma = 2$ boundaries originate from the starting WC powder [10,16,17,20]. During sintering, the fraction of $\Sigma = 2$ boundary area of the total WC/WC boundary area decreases [17,21,22], and the $\Sigma = 2$ boundaries are to some extent eliminated in the sintering process [17,21]. Before sintering, the $\Sigma = 2$ boundaries are usually curved, and thus have a varying character of twist and tilt, but they straighten into pure twist boundaries in the sintering process [21]. A majority of $\Sigma = 2$ boundaries in the sintered material are therefore twist boundaries [15,18,23].

Since the slip planes in WC are $\{10\bar{1}0\}$ [1], two grains joined in a 90°$[10\bar{1}0]$ twist boundary do not share any common slip plane across the boundary [24]. A $\Sigma = 2$ twist boundary could thus form a barrier for dislocation movement during plastic deformation of the WC skeleton. In Ref. [21], it was argued that the $\Sigma = 2$ twist boundaries appear during the production of WC powder and upon the severe plastic deformation during subsequent milling they curve. Furthermore, it has been observed that the fraction of twist boundaries of the $\Sigma = 2$ boundaries decreases close to the cutting edge of a deformed cutting tool insert [25] as well as in a material deformed by three-point bending [26]. These observations indicate that $\Sigma = 2$ twist boundaries within the WC grains curve under load and thereby accomodate a part of the plastic deformation. A complex defect structure, which may be due to the interaction of a $\Sigma = 2$ twist boundary with a dislocation of WC, has also been identified in a recent high resolution transmission electron microscopy (HRTEM) study [14].

A detailed knowledge of the atomic structure, the chemical content and the energetics of the $\Sigma = 2$ boundaries is therefore

* Corresponding author.
E-mail address: goran.wahnstrom@chalmers.se (G. Wahnström).

http://dx.doi.org/10.1016/j.commatsci.2014.11.024
0927-0256/

necessary for understanding their effect on the plastic deformation of the material as well as their behavior during sintering. It is well-known that Co segregates to most WC/WC boundaries in sub-monolayer proportion [4,7,12,13], although some special boundaries, notably the $\Sigma = 2$ twist boundary, have been found to contain no segregants [7]. Several HRTEM studies of the atomic structure of the $\Sigma = 2$ twist boundary have been made [5,7,8,14] showing a semicoherent structure consistent in average with a periodicity of $41a \approx 42c$. The misfit structure has been found to be comprised of monolayer steps on the interfacing $\{10\bar{1}0\}$ planes.

A previous density functional theory (DFT) study of the $\Sigma = 2$ twist boundary gave a very low grain boundary energy of only 0.02 J/m^2 under the coherent boundary approximation ($c = a$) [9]. This is much lower than the grain boundary energies of more general WC/WC boundaries, including $\Sigma = 2$ tilt boundaries, which lie between 2 and 3 J/m^2 [11,27]. In the previous DFT work, no explicit account of the $c \neq a$ misfit was made nor was Co segregation considered [9]. In this paper, we first extend the previous DFT calculations and calculate the energy of the coherent $\Sigma = 2$ twist boundary as well as of other $\Sigma = 2$ and $\Sigma = 1$ boundaries with $\{10\bar{1}0\}$ boundary planes. The DFT calculations are done in the GGA-PBE approximation, and further details are given in [28].

Then, we determine the structure and energetic contribution of the twist boundary misfit using a Peierls–Nabarro (PN) model for semicoherent interfaces. The model was previously used by us to calculate the interface energy and structure of the semicoherent Fe/VN interface [29,30]. It is essentially a continuum model, the input of which is obtained from DFT calculations of small supercells. To assess its accuracy, we also use input from calculations with a classical analytical bond-order potential (ABOP) [31]. Owing to its computational simplicity, the ABOP allows for a direct comparison between model and full-scale molecular statics (MS) simulations. Finally, we assess the tendency of Co segregation in the studied $\Sigma = 2$ boundaries.

2. Method

2.1. Geometry

WC has a hexagonal unit cell with an atomic basis that can be chosen as W at $(0,0,0)$ and C at $(2/3,1/3,1/2)$ (or, alternatively, $(1/3,2/3,1/2)$) with respect to hexagonal lattice vectors $\boldsymbol{a}_1, \boldsymbol{a}_2$ and $\boldsymbol{c}$. In Fig. 1, a projection along the basal $[0001]$ direction of a small WC hexagon bounded by prismatic $\{10\bar{1}0\}$ surfaces is depicted. Owing to the non-centrosymmetric structure of WC, there are two structurally different $\{10\bar{1}0\}$ facets, which we denote S and T as in Refs. [32,33]. These differ in the sequence of W–C interplanar distances as measured from the grain core towards the surface along the surface normal. With $d = a_{WC}\sqrt{3}/2$ being the $(10\bar{1}0)$ spacing, the sequences are

$$\mathrm{S}: \text{core} \rightarrow \text{W layer}, 2d/3\text{spacing}, \text{C layer}, d/3\text{spacing}, \text{W layer} \rightarrow \text{surface}$$
$$\mathrm{T}: \text{core} \rightarrow \text{W layer}, d/3\text{spacing}, \text{C layer}, 2d/3\text{spacing}, \text{W layer} \rightarrow \text{surface}$$

In turn, the S and T facets have either W- or C-termination. As in Ref. [34,35], we denote these terminations C-I, C-II, W-I and W-II, where the Roman numeral indicates whether the distance between the two atomic planes closest to the surface is $d/3$ or $2d/3$.

There are three ways of constructing structurally inequivalent $\Sigma = 2$ boundaries in which both crystals have $\{10\bar{1}0\}$ boundary planes: S/S, S/T and T/T. The CSL is found by finding coincident lattice points, and for the S/T boundary one can use either W or C atomic positions to construct the CSL, but this is not possible for S/S or T/T. Only the S/T combination corresponds to a $90°[10\bar{1}0]$ pure twist boundary. The S/S and T/T boundaries can in fact be described by the misorientations $104.48°[4\bar{2}\bar{2}3]$ and $104.48°[4\bar{2}\bar{2}\bar{3}]$, respectively [3]. However, in most EBSD analyses, a hexagonal symmetry is assumed for WC, in which case these three combinations are not differentiated. Therefore, all three will here be studied to ascertain that the twist boundary indeed is associated with the lowest energy. Typical atomic structures of the different $\Sigma = 2$ boundaries are depicted in Fig. 2.

It is also possible to construct perfectly coherent $\Sigma = 1$ boundaries with $\{10\bar{1}0\}$ boundary planes by choosing a misorientation of $60°[0001]$. In this orientation, the lattices of the grains coincide perfectly, but the atomic bases are different with e. g. C changing from $(2/3,1/3,1/2)$ to $(1/3,2/3,1/2)$ across the boundary. Depending on the choice of boundary planes, these boundaries are of S/S or T/T type. $\Sigma = 1$ boundaries have been shown to exist in sintered WC–Co [10] and, for comparison, these will also be included in the present study. Atomic structures of the modeled $\Sigma = 1$ boundaries are depicted in Fig. 3.

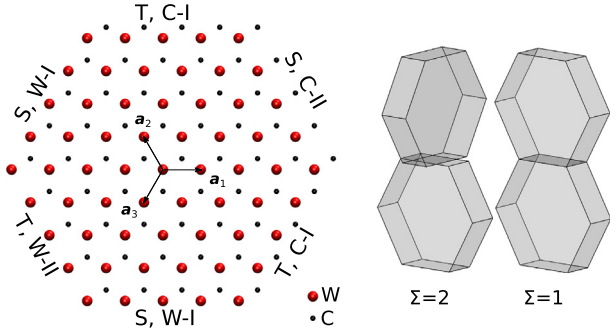

Fig. 1. Left: A projection along the basal $[0001]$ direction of a small WC hexagon showing different kinds of prismatic $\{10\bar{1}0\}$ facets and terminations. Right: A schematic diagram of hexagonal grains in $\Sigma = 2$ and $\Sigma = 1$ relations joined with $\{10\bar{1}0\}$ boundary planes.

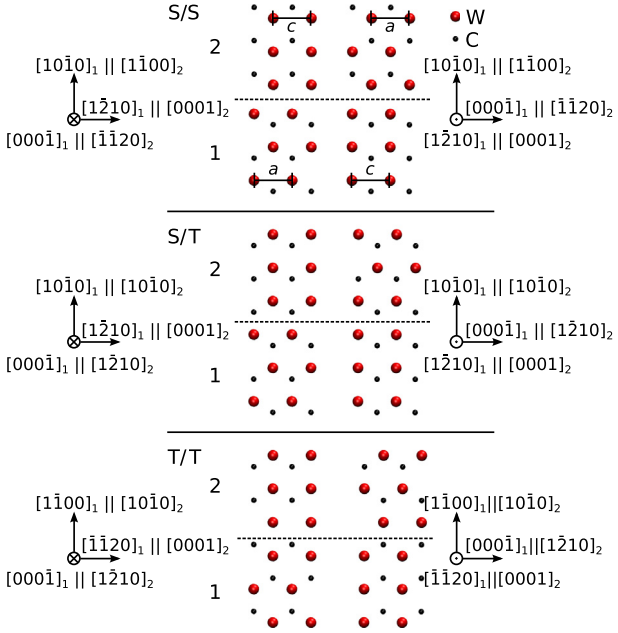

Fig. 2. Atomic structures of $\Sigma = 2$ boundaries as seen from two mutually orthogonal directions. The dashed lines mark the grain boundary planes. The depicted terminations and relative translations correspond to the ones of lowest energy in the coherent approximation ($a = c$).